

PACS numbers: 42.62.–b; 21.10.Hw

Broad-band laser optical pumping of Rb for the creation of nuclear polarisation in ^{3}He

N N Kolachevskiĭ, A A Papchenko, Yu V Prokof'ichev,
V R Skoĭ, I I Sobel'man, V N Sorokin

DOI: 10.1070/QE2000v030n01ABEH001664

Abstract. **A large volume (30 cm^3) of dense (up to 10^{15} cm^{-3}) Rb vapour was pumped optically by a high-power laser diode array. The conditions for the propagation of high-power broad-band optical pump radiation through an optically dense medium were examined. A spectroscopic method was developed for determination of the polarisation of Rb. The dependence of the polarisation of Rb on its vapour pressure was investigated at buffer gas pressures of 1, 8, and 13 bar. Under optimal conditions a 15-W diode laser made it possible to polarise at least 10^{18} of ^{3}He atoms per second during collisions between Rb and ^{3}He atoms, sufficient for the creation of an efficient neutron polariser.**

1. Introduction

Spin-polarised nuclei have a wide range of potential applications in fundamental physics. Studies in this field have been going on for a long time [1] and there is special interest in spin-polarised rare-gas nuclei (^{4}He, ^{129}Xe, and ^{131}Xe). For the latter, it is possible to ensure conditions such that the longitudinal relaxation time reaches several hours. This permits the attainment of a strong nuclear polarisation by its accumulation over a long period. High-pressure spin-polarised gases are used in experiments on polarised nuclei [2], electrons and ions [3], and also in medicine in the tomographic study of lung ventilation [4].

We plan to employ a polarised ^{3}He target as a thermal-neutron beam polariser in T-invariance test experiments on polarised ^{131}Xe (KaTRIn Project) [5]. The cross section σ for the reaction between a neutron and ^{3}He, resulting in the formation of tritium, is $\sim 10^{-24}$ cm^2 when the polarisations of the neutron and ^{3}He are parallel and $\sim 10^{-21}$ cm^2 when they are antiparallel. This means that efficient polarisation of a neutron beam requires a polarised target with an ^{3}He pressure of approximately 10 bar and a length of several centimetres. For real dimensions of neutron beams, this corresponds approximately to 1 litre of a gas, 50% polarised under normal conditions.

The technology for the creation of nuclear polarisation in ^{3}He has been thoroughly investigated and may be subdivided into three main approaches: (1) direct optical orientation of ^{3}He atoms in the metastable state [6]; (2) collisional transfer of electron-spin polarisation from an optically polarised alkali metal atom to a ^{3}He nucleus [7]; (3) polarisation in strong magnetic fields at low temperatures [8]. An Rb atom, with the rate constant of the transfer of electron-spin polarisation to the nuclear-spin polarisation of ^{3}He amounting to $\langle\sigma_{\mathrm{RbHe}}v\rangle = 1.2 \times 10^{-19}$ cm^3 s^{-1}, is widely used in the polarisation of rare-gas nuclei. In order to achieve a strong nuclear polarisation ($P_{\mathrm{He}} \sim 1$), the characteristic time of the transfer of polarisation to helium $\tau_{\mathrm{RbHe}} = (\langle\sigma_{\mathrm{RbHe}}v\rangle[\mathrm{Rb}])^{-1}$ should be appreciably shorter than the decay time of the ^{3}He nuclear-spin polarisation which, according to experimental data, is 10 – 40 h for aluminosilicate glass cells. This condition is satisfied ($\tau_{\mathrm{RbHe}} = 3$ h) when the rubidium vapour concentration is $[\mathrm{Rb}] = 10^{15}$ cm^{-3}.

Since a strong nuclear polarisation P_{He} is attainable for an electron polarisation $\bar{P}_{\mathrm{Rb}}$ close to unity, a high-power polarising radiation (pump) corresponding to a resonant transition in the Rb atom is essential. Titanium-doped sapphire lasers [2], dye lasers [9], and diode lasers [7], tuned to the $D1$ rubidium resonance line (795 nm), are used as the optical pump sources. A typical width of the emission spectra of such lasers amounts to several gigahertz and is usually less than the width of the Rb line collision-broadened by helium.

Estimates show [7] that, in order to attain high values of $\bar{P}_{\mathrm{Rb}}$, it is necessary to have at one's disposal a laser pump ensuring absorption by rubidium vapour of 0.2 W cm^{-3} at concentrations $[\mathrm{Rb}] = 10^{15}$ cm^{-3}. High-power diode-laser systems, consisting of arrays of selected laser diodes with a total power up to 30 W in a spectral range about 3 nm wide (Opto Power Corp., 3321 E.Global Loop, Tuscon, AZ85706), are now available. In contrast to the Ti : sapphire systems, such diode-laser arrays do not require an expensive pumping system, are reliable and stable, and are highly efficient. However, for this width of the emission spectrum, one may expect the pumping efficiency and $\bar{P}_{\mathrm{Rb}}$ to depend significantly on the absorption conditions.

We used a diode-laser array to assemble an experimental setup for ensuring a strong electron polarisation ($\bar{P}_{\mathrm{Rb}} = 0.8$ – 0.9) of large volumes (up to 30 cm^3) of dense rubidium vapour and for recording the NMR spectra of spin-polarised ^{3}He nuclei. The propagation of broad-band polarising laser radiation through Rb vapour was investigated in detail.

2. Optical pumping by laser radiation

We shall examine the propagation of circularly polarised pump radiation with a spectral density $I(\omega)$ through a cell of length L containing Rb vapour (a natural mixture of ^{85}Rb

N N Kolachevskiĭ, A A Papchenko, I I Sobel'man, V N Sorokin
P N Lebedev Physics Institute, Russian Academy of Sciences, Leninskiĭ prospekt 53, 117924 Moscow, Russia;
Yu V Prokof'ichev, V R Skoĭ I M Frank Neutron Physics Laboratory, Joint Institute of Nuclear Research, Dubna, Moscow Province, 141980 Russia

Received 21 June 1999
Kvantovaya Elektronika **30** (1) 81 – 86 (2000)
Translated by A K Grzybowski

and ^{87}Rb) at a temperature T, as well as high-pressure gaseous ^{3}He. The system of magnetic Rb sublevels, corresponding to the $D1$ resonance emission line, is illustrated in Fig. 1. The relative populations are designated in the figure by n_0 (the light-absorbing sublevel), n_1 (the pumped sublevel), and n_2, n_3 (upper sublevels); $n_0 + n_1 + n_2 + n_3 = 1$; $W_{\rm opt}$ is the probability of the absorption of a pump photon (per unit time); A is the probability of the relaxation of excitation, including the probability of the radiative decay $\Gamma_{\rm rad}$; W^* and W are the probabilities of collisional mixing of the upper and lower magnetic sublevels. The probability of spin relaxation in rubidium – rubidium collisions, which enters into W as a component, is designated by W_2. Under the experimental conditions, the upper magnetic sublevels are hardly populated ($n_2 + n_3 \ll 1$) and by virtue of the high probability of mixing W^*, the equality $n_2 = n_3 = (1/2)n^*$ (where n^* is the population of the upper level) is valid to a high decree of accuracy. In practice, this system should be regarded as a three-level scheme.

Furthermore, summation over the upper magnetic sublevels is implied in the probabilities of all the processes involving the upper level. In the steady state, we have

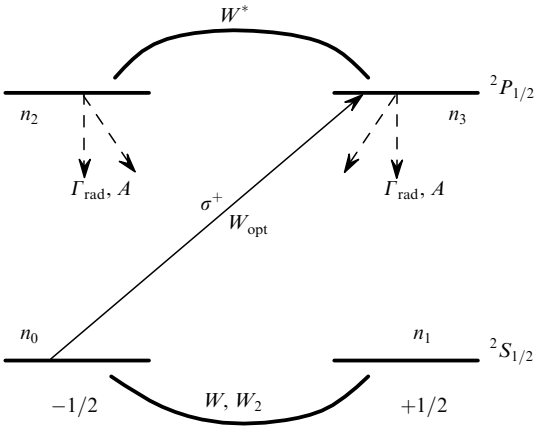

Figure 1. Rb levels participating in optical pumping.

$$W_{\rm opt} n_0 = A n^*, \tag{1}$$

and the absorption probability is expressed in terms of the spectral laser-radiation density:

$$W_{\rm opt} = \int I(\omega)\sigma(\omega)\,{\rm d}(\omega) \quad ,(2)$$

The absorption cross section $\sigma(\omega)$ has a Lorentzian profile:

$$\sigma(\omega) = \frac{\sigma_0}{1 + 4(\omega - \omega_0)^2/\Gamma^2}\,, \tag{3}$$

where Γ is the resonance line width; ω_0 is the resonance transition frequency; σ_0 is the absorption cross section at the maximum. At high ^{3}He pressures, the collisional broadening of the $D1$ line (the collisional broadening constant in ^{3}He under normal conditions is 18 GHz bar^{-1}) predominates appreciably over the natural width (6 MHz) and over the Doppler broadening at $T = 473$ K (250 MHz). The absorption cross section at the maximum is $\sigma_0 = 4.24 \times 10^{-13}$ cm^2 at the helium pressure of 760 Torr and is inversely proportional to the increase in the helium pressure.

In the steady state, the population of the absorbing sublevel is

$$-W_{\rm opt} n_0 + \tfrac{1}{2} A n^* - R(n_0 - n_1) = 0\,, \tag{4}$$

where R is the total probability of all the processes leading to mixing of the lower magnetic sublevels, including the transfer of electron-spin polarisation to a helium nucleus. In the above equation no account is taken of processes such as the radiation trapping and relaxation collisions between polarised and excited rubidium atoms. We note that the relaxation of the electron polarisation in Rb – Rb collisions leads to a contribution, in expression (4), quadratic in the concentration [Rb], but the nonlinearity is eliminated by virtue of the relationship $n_0 + n_1 \approx 1$. From expressions (1) and (4), we obtain the population of the absorbing sublevel:

$$n_0 = \frac{1}{2 + W_{\rm opt}/2R} \tag{5}$$

and the degree of polarisation of rubidium atoms in the ground state:

$$P_{\rm Rb} = \frac{W_{\rm opt}/2R}{2 + W_{\rm opt}/2R} = \frac{W_{\rm opt}}{4R + W_{\rm opt}}\,. \tag{6}$$

In the expression for $P_{\rm Rb}$, only R depends explicitly on A. The radiative transition from the upper to the lower level generates photons with a polarisation different from the polarisation of the pump radiation. In its turn this leads to an additional Rb depolarisation mechanism. Nitrogen, at a pressure of about 100 Torr, was added to the cell in order to prevent radiation trapping. The cross section of the $6P_{1/2} - 5S_{1/2}$ transition quenching of Rb by nitrogen is 5.8×10^{-15} cm^2 and, under the indicated conditions, such quenching leads to a contribution of $\sim$75 MHz to the line width, which exceeds the radiative width by a factor greater than 10.

The number of photons absorbed by rubidium atoms per unit time is $W_{\rm opt} n_0$, whereas the number of photons re-emitted during this period is $W_{\rm opt} n_0 \Gamma_{\rm rad}/A$, which is smaller by the factor $\Gamma_{\rm rad}/A$. Some of the re-emitted photons may be absorbed by polarised atoms, leading thereby to the depolarisation of Rb atoms. At the quenching-impurity concentration indicated above, this channel of relaxation of the atomic polarisation may be neglected. The spin-exchange collisions of the polarised rubidium atoms in the ground state with the depolarised excited atoms may serve as yet another spin-relaxation mechanism. However, the presence of the quenching impurity reduces the population of the excited sublevels given by expression (1), which in its turn reduces the probability of the process in question. The small amount of the nitrogen impurity has an insignificant influence on the line width Γ, so that the broadening constant of the Rb $D1$ line is 14 GHz bar^{-1}.

We shall introduce a coordinate x along the direction of propagation of radiation, measured from the entry window of the cell. We shall examine the dependence of the degree of polarisation of rubidium on x. We shall also neglect diffusion both in the interior of the cell and in the wall layer near the 'entry' window ($x = 0$). Taking into account the absorption of light described by the expression

$$\frac{{\rm d}I(\omega, x)}{{\rm d}x} = -I(\omega, x)\sigma(\omega) n_0(x)[{\rm Rb}]\,, \tag{7}$$

and expressions (2) and (5), we obtain a closed system of equations. This system was solved numerically for a cell of length L. The following parameters were monitored in

the calculation: the spectral density of the transmitted radiation $I_{out}(\omega) = I(\omega, L)$, the distribution of the degree of polarisation of rubidium along the length of the cell $P_{Rb}(x)$, and the average degree of polarisation P_{Rb} defined by the formula

$$\bar{P}_{Rb} = \frac{1}{L}\int_0^L P_{Rb}(x)\,dx\,. \tag{8}$$

It was established that the average degree of polarisation can be obtained very accurately when the spectral distributions of the intensities of the incident and transmitted light are known:

$$I_{out}(\omega) = I(\omega, 0)\exp\left\{-\sigma(\omega)\frac{1-\bar{P}_{Rb}}{2}[Rb]L\right\}. \tag{9}$$

3. Experimental setup

Fig. 2 shows the optical experimental system for the generation and recording of the electron polarisation in Rb. The Opto Power Corporation OPC-A105-795-FCPS laser diode system (henceforth simply referred to as the laser) consists of an array of 23 laser diodes, each of which is coupled to an optical fibre. When operating, the laser emits cw radiation of 15 W power through an optical-fibre end face 1.55 mm in diameter. The angular distribution of the radiation is 12° wide (at the $1/e^2$ level). The dependence of the spectral characteristics of the laser on the diode current and temperature was studied in detail with the aid of a 1.6-metre spectrograph (resolution 0.05 nm) incorporating a $\frac{1}{3}$-inch CCD video camera of the MTV-361 CM type. Near the operating point (795 nm), the centre of the laser spectrum shifts at the rates of 0.33 nm A^{-1} and 0.28 nm K^{-1}, respectively, when the current and temperature are varied. Then 80% of the laser power corresponds to a 2.4 nm band near the Rb absorption line (a typical profile of the laser spectrum can be seen in Fig. 3).

The laser beam is expanded by a lens and is split by a polarisation cube into two linearly polarised beams, the circular polarisation of which is generated by Fresnel rhombs. The beams converge on the cell (the angle between the beam centres is less than 4°), where they have a diameter of 2–4 cm (depending on the alignment). The radiation transmitted through the central part of the cell is guided by an optical fibre to a spectrometer which records the transmission spectrum of the cell in the spectral range 792.7–797.3 nm.

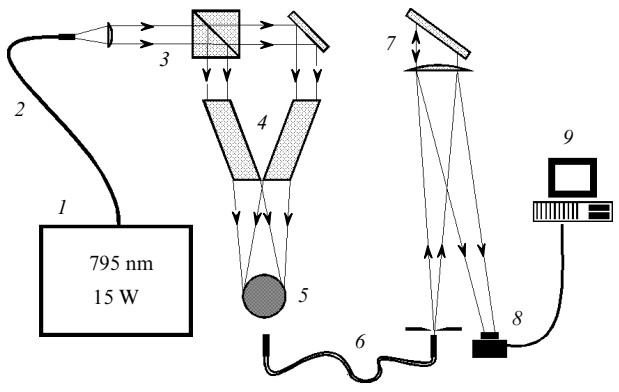

Figure 2. Optical experimental setup: (*1*) diode laser; (*2*) laser optical fibre with a beam expander; (*3*) polarising cube; (*4*) Fresnel rhombs; (*5*) pumped cell; (*6*) detecting optical fibre; (*7*) spectrograph; (*8*) video camera; (*9*) computer.

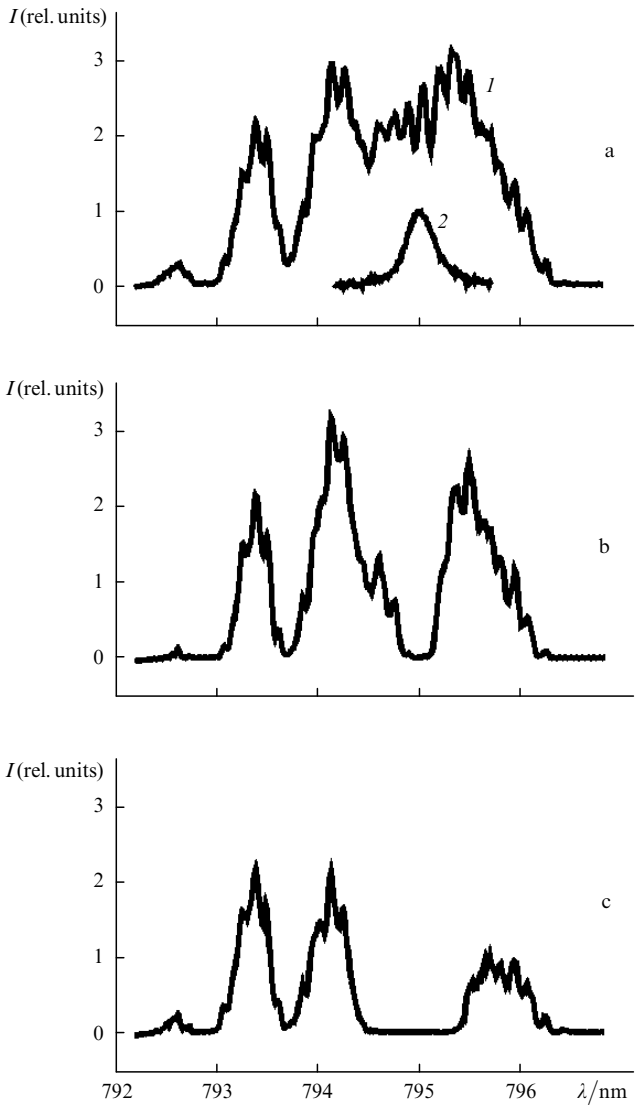

Figure 3. Laser emission spectra (*1*) and Rb absorption lines [in the linear region (*2*)] (a) and spectra of the radiation transmitted through the cell with Rb in the presence (b) and absence (c) of the magnetic field B_0.

The experiments were performed on three spherical aluminosilicate glass (Corning 1720) cells 1.5, 4, and 3 cm in diameter, filled with ^{3}He under pressures of 1, 8, and 13 bar, respectively. The helium pressure in the cells 3 and 4 cm in diameter was monitored on the basis of the width Γ of the rubidium resonance line determined from the absorption spectra in its vicinity. A stabilising $B_0 = 20$ G magnetic field, directed along the laser pump beam, was generated by Helmholtz coils 1.5 m in diameter. In the absence of the field B_0 the laboratory magnetic field is $B_{lab} = 0.38$ G, perpendicular to the laser beam axis and leading to precession of the electron spins and to decay of the polarisation.

The cells were heated by hot air to temperatures of 150 °C–200 °C, corresponding to the Rb concentrations from 10^{14} to 10^{15} cm^{-3}. The relationship between the Rb vapour concentration and the temperature T is described by a semiempirical formula (the Killian formula):

$$[Rb] = \frac{1}{T}10^{26.41-4132/T}\,, \tag{10}$$

where the absolute temperature T is expressed in kelvins [10], while [Rb] is in reciprocal cubic centrimetres. The Rb concentration was determined from the absorption spectra in the absence of the field B_0. Since the line width Γ was known, we could determine the absorption coefficient at the maximum by fitting the spectrum described by expression (9) to the experimentally recorded spectrum. A typical experimental error was 15%, increasing to 25% at high temperatures when more than 85% of the incident radiation was absorbed. Rubidium became polarised when the field B_0 was applied, which reduced the number of absorbers and causes bleaching (Fig. 3). Knowing the ratio of the absorption coefficients at the maximum in the presence and absence of the field B_0, it was possible to calculate the electron polarisation $\bar{P}_{\mathrm{Rb}}$ averaged over the cell diameter.

Fig. 4 presents experimental and theoretical dependences of $\bar{P}_{\mathrm{Rb}}$ on [Rb] for the cells 1.5 and 4 cm in diameter at power densities of the incident radiation of 1 and 0.5 W cm^{-2}. The dependences for the cell 3 cm in diameter are on the whole the same as for the cell 4 cm in diameter and are not shown in Fig. 4. We note that, for the 3-cm cell, $\bar{P}_{\mathrm{Rb}}$ exceeds somewhat $\bar{P}_{\mathrm{Rb}}$ for the 4-cm cell at the same Rb concentrations and reaches 0.8 for $[\mathrm{Rb}] = 6 \times 10^{14}$ cm^{-3}.

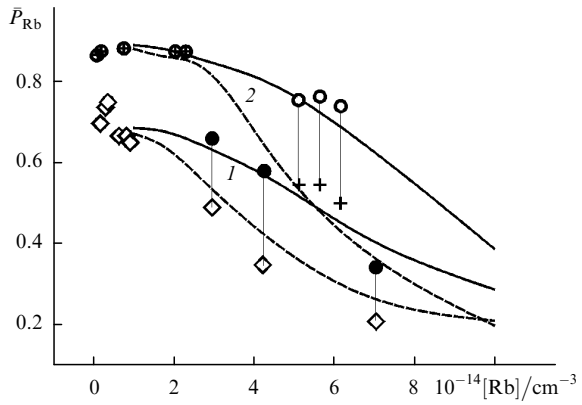

Figure 4. Experimental and calculated dependences of $\bar{P}_{\mathrm{Rb}}$ on [Rb] for the cells 1.5 cm (*1*) and 4 cm (*2*) in diameter and for the intensities of 1 W cm^{-2} and 0.5 W cm^{-2} (dashed curves). The experimental points corresponding to the same temperature but at different intensities are joined by vertical lines.

For the cells 3 and 4 cm in diameter (the high-pressure cells), the average degree of polarisation in a large volume (up to 30 cm^3) remains 0.8 up to the Rb concentration of 6×10^{14} cm^{-3}, sufficient for the efficient transfer of the polarisation to the ^{3}He gas. About 90% of the power of the laser with a spectral width of $\sim$3 nm (which corresponds to $\sim 6\Gamma$ for the cell 4 cm in diameter and $\sim 10\Gamma$ for the cell 3 cm in diameter) is then used to generate the polarisation.

The polarisation in the spherical cell 1.5 cm in diameter (helium pressure 1 bar) decreases rapidly with the increase in the Rb concentration, which can be explained by the narrowness of the absorption line and hence by the small fraction of the absorbed light. For the low-pressure cells, this may be compensated by increasing the laser radiation intensity and the cell length, because the width of the absorption spectrum is $\Delta\omega_{1/2} \propto ([\mathrm{He}]L)^{1/2}$. However, spherical cells were preferred in our investigation first, because of the ease of fabrication and, second, because of the ease of filling their volume with laser radiation without formation of 'dark' unpolarised regions. Their disadvantage is a depolarisation of the peripheral part of the beam crossing the interior of the cell.

High ^{3}He pressures are needed to increase the absorption of the neutron beam and the fraction of optical flux consumed in polarising the nuclei. Fig. 5 presents the calculated distribution of the polarisation in the cell 5 cm long, obtained for the power density of the incident radiation of 1 W cm^{-2} (beam diameter 3 cm) at the Rb concentration of 6×10^{14} cm^{-3} and various helium pressures. An increase in the helium pressure evidently leads to a rise in the average polarisation $\bar{P}_{\mathrm{Rb}}$. At high helium pressures, there are a number of competing processes [11], which limit the rise of $\bar{P}_{\mathrm{Rb}}$: partial overlap of the $D1$ and $D2$ resonance lines as a consequence of broadening, relaxation of the polarisation owing to the spin-exchange and spin–orbit interactions with ^{3}He, and three-body Rb–He–He collisions. At the Rb concentration of 6×10^{14} cm^{-3}, the rate of relaxation of the Rb polarisation due to three-body collisions becomes equal to the rate of depolarisation due to Rb–Rb collisions at helium pressures of $\sim$10 bar [12]. From the standpoint of practical applications of polarised ^{3}He, it would therefore be preferable not to use helium pressures more than 15–20 bar.

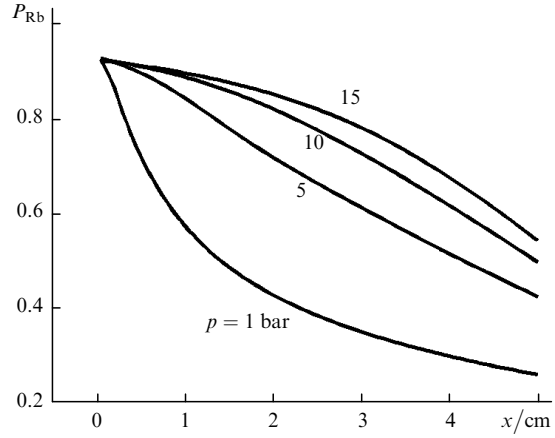

Figure 5. Calculated dependences of P_{Rb} on x for different ^{3}He pressures and for the laser intensity of 1 W cm^{-2} at the Rb concentration of 6×10^{14} cm^{-3}.

4. Results

A schematic diagram of the setup for detection of the nuclear polarisation P_{He} in ^{3}He is shown in Fig. 6. The relative measurements of P_{He} were made on the basis of NMR spectra recorded by the fast adiabatic-passage method. A cell was placed in a homogeneous static magnetic field $B_0 = 22$ G generated by a system of Helmholtz coils 1.5 m in diameter. The field inhomogeneity was 5×10^{-4} in the central region 5 cm in diameter and 20 cm long. Its temporal instability was also 5×10^{-4}. A high field homogeneity was needed to ensure a long lifetime of the nuclear polarisation.

An rf field $\boldsymbol{B}_1$ (orthogonal to $\boldsymbol{B}_2$) at the frequency of 78 kHz was generated by a system of Helmholtz coils 0.7 m in diameter. A sawtooth field pulse with an amplitude of 3 G was superimposed on the stabilising field $\boldsymbol{B}_0$, so that the resonance condition (gyromagnetic ratio $\gamma_{^3\mathrm{He}} = 3.24$ kHz G^{-1}) should hold for the nuclear spins. The amplitude B_1 and the pulse duration were chosen so that the fast

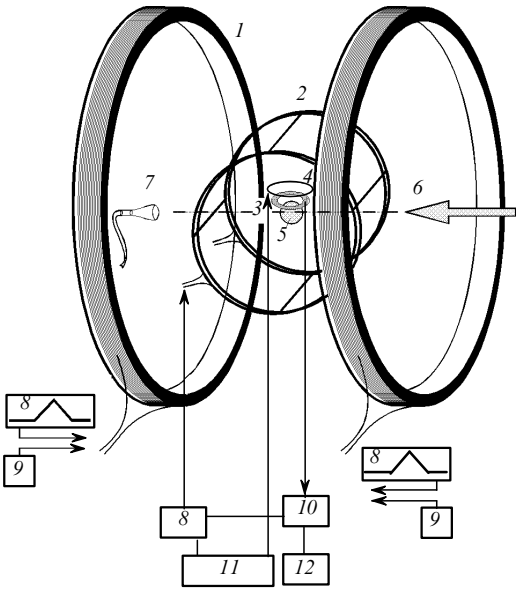

Figure 6. Schematic diagram of the apparatus for the recording of NMR spectra by the fast adiabatic-passage method: (*1*) Helmholtz coil system for the generation of a stabilised field B_0 (diameter 1.5 m); (*2*) Helmholtz system for the generation of an rf field B_1 (diameter 0.7 m); (*3*) sensor coil; (*4*) compensating coil; (*5*) test sample; (*6*) direction of the laser beam; (*7*) end face of a detecting optical fibre; (*8*) oscillator; (*9*) power supply; (*10*) lock-in detector; (*11*) amplitude – phase control unit; (*12*) digital oscilloscope.

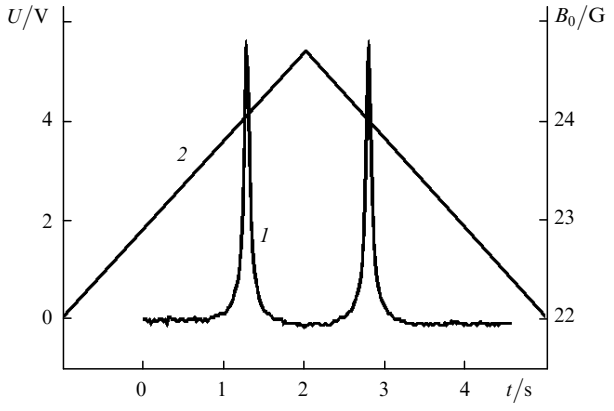

Figure 7. Typical NMR oscillogram (*1*) and sawtooth profile (*2*) of the magnetic field B_0 used to scan the spectrum.

adiabatic-passage conditions should be fulfilled [13]. A sensor coil (tuned to a resonance) and a compensating coil, with their axes orthogonal to the vectors $\boldsymbol{B}_0$ and $\boldsymbol{B}_1$, were located near the investigated volume. The signal induced in the sensor coil was sent to a lock-in detector and displayed on the screen of a THS730A digital oscilloscope. The system sensitivity was $\sim 5 \times 10^4$ V G^{-1}. The noise was determined by the rf interference and vibrations and it was equivalent to a 100 mV signal. A typical NMR spectrum is presented in Fig. 7. The absolute value of P_{He} was estimated from calculations of the geometrical factor (the sensor-coil fill factor).

The NMR spectra were used to estimate P_{He} and to measure the polarisation lifetime. For the sample 1.5 cm in diameter, the polarisation lifetime reached several hours ($P_{\mathrm{He}} \sim 40\%$). Under the conditions in the cell 4 cm in diameter, our system made it possible to obtain about 10^{18} polarised ^{3}He atoms per second, i.e. the polarisation of a single nuclear spin was attained on absorption of about 60 photons. Such a polarisation rate is sufficient to generate a strong polarisation P_{He} in a volume of the order of 100 cm^3, divided into a 'hot' pumped part and a 'cold' part free of Rb vapour, and designed for the accumulation of nuclear polarisation.

It was confirmed experimentally (in the cell 3 cm long) that in such a system it is possible to maintain a high temperature difference (150 K – 200 K), so that the Rb concentration in the 'cold' part is negligible. Under these conditions, almost the entire Rb remains in the 'hot' part. The external view of the cell 3 cm in diameter is presented in Fig. 8. The attainment of a high P_{He} in such a cell requires a relaxation time about 10 h, which is attainable for a high chemical purity of ^{3}He (the content of paramagnetic impurities no more than 10^{-6}) and after a special treatment of the aluminosilicate-glass cell walls.

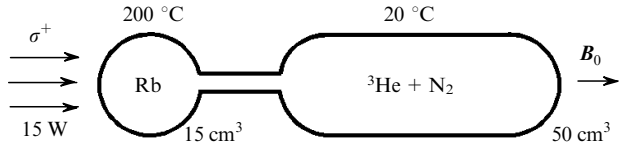

Figure 8. Schematic diagram of a two-component cell.

5. Conclusions

An experimental setup for the generation and investigation of polarised ^{3}He was assembled as part of the KaTRIn Project to test the T-invariance in experiments with polarised ^{131}Xe. The ^{3}He nuclei were polarised in collisions with polarised Rb atoms. The electron polarisation of the Rb vapour was induced by optical pumping with circularly polarised radiation of a 15-W diode laser system and the radiation spectral width of 3 nm. The efficiency of the utilisation of the broad-band radiation of this system in spherical cells increased with increase in the buffer gas pressure and reached 90% at the helium pressure of 10 bar.

A spectroscopic method was developed for determination of the average polarisation of a dense Rb vapour from the absorption spectra of the pump radiation. In a volume of 30 cm^3, 70% – 80% electron polarisation of Rb was achieved when the concentration of rubidium was 6×10^{14} cm^{-3}. A model was proposed for the propagation of high-power polarising pump radiation through an optically dense medium. A signal from the polarised ^{3}He nuclei was detected with the aid of NMR spectra and typical rise and decay times of the polarisation were determined for different cells. According to our estimates of the rate of increase of the nuclear polarisation, our laser system can polarise at least 10^{18} nuclei per second, which is sufficient to construct a thermal-neutron polariser.

Acknowledgements. The authors are grateful to S I Kanorskiĭ for constructive suggestions. The study was carried out with the support of the Russian Foundation for Basic Research (Grant No. 96-15-96438), the Arizona State University, the Department of Defence of the USA, and the 'Fundamental Optics and Spectroscopy' Research and Teaching Centre as part of the 'Integration' programme.

References

1. Happer W *Rev. Mod. Phys.* **44** 169 (1972)
2. Johnson J R, Thompson A K, Chupp T E, et al. *Nucl. Instrum. Methods Phys. Res. A* **356** 148 (1995)
3. Rutherford G H, Ratliff J M, Lynn J G, et al. *Rev. Sci. Instrum.* **61** 1460 (1990)
4. Ebert M, Grossman T, Heil W, Otton W E, et al. *Lancet* **347** 1297 (1996)
5. Scoy V R, Procofichev Yu V, Kolachevsky N N, Sorokin V N *Nucl. Instrum. Methods Phys. Res. A* **402** 322 (1997)
6. Eckert G, Heil W, Meyerhoff M, et al. *Nucl. Instrum. Methods Phys. Rev. A* **320** 53 (1992)
7. Chupp T E, Wagshul M E, Coutler K P, et al. *Phys. Rev. C* **36** 2244 (1987)
8. Laloo F, Leduc M, Nacher P J, et al. *Usp. Fiz. Nauk* **147** 433 (1985) [*Sov. Phys. Usp.* **28** 941 (1985)]
9. Cates G D, Fitzgerald R J, Barton A S, et al. *Phys. Rev. A* **45** 4631 (1992)
10. Killian T J *Phys. Rev.* **27** 578 (1926)
11. Papchenko A A, Sobel'man I I, Yukov E A, Preprint No. 124 (Moscow: Lebedev Physics Institute, Russian Academy of Sciences, 1989)
12. Larson B, Hausser O, Delheij P P J, et al. *Phys. Rev. A* **44** 3108 (1991)
13. Wagshul M E, Chupp T E *Phys. Rev. A* **49** 3854 (1994)